Advances in Engineering Research : Possibilities and Challenges
ISSN Print: 3079-5192
ISSN Online: 3079-5206
https://doi.org/10.63313/AERpc.9005

Wind Environment Simulation Analysis of Office Buildings Based on PHOENICS—A Case Study of Mianyang City Office Complex

Yuzhenru Sun. Yang Li. Baofeng Liang and Jun Qin
School of Architecture, Southwest Minzu University, Chengdu 610225, PR China

How to cite this paper: Sun, Y., Li, Y., Liang, B., & Qin, J. (2025). Wind Environment Simulation Analysis of Office Buildings Based on PHOENICS—A Case Study of Mianyang City Office Complex. *Advances in Engineering Research: Possibilities and Challenges*, 1(1), 46-60. ISSN Print: 3079-5192; ISSN Online: 3079-5206.
https://doi.org/10.63313/AERpc.9005
Published: 2025-03-17

Abstract

This electronic investigates the wind environment optimization of office build-ing clusters in hot-summer and cold-winter regions through computational fluid dynamics simulations under dual-season conditions. A three-dimensional nu-merical model encompassing a 1200-meter extended area was established, em-ploying high-precision meshing and advanced turbulence models to analyze wind speed distribution at pedestrian height under winter northwest prevailing winds and summer southeast wind-induced surface pressure gradients. Results reveal that winter leeward zones develop maximum wind speeds of 7.2 m/s, with 18.3% of the area exceeding standard limits. Summer southeast facades ex-hibit significant negative pressure coefficients of 0.82, reducing natural ventila-tion efficiency to 1.2 air changes per hour. Through extreme pressure differential analysis, primary entrances are recommended for placement in southeast re-gions with pressure gradients below 0.3 to mitigate winter wind disturbances. The optimized design enhances site thermal comfort by 38% and achieves an-nual energy savings of 12.7 kWh/m^2, providing quantitative benchmarks for green building wind environment assessment and advancing climate-responsive urban design practices.

Keywords

Office Buildings; CFD Wind Environment Analysis; Passive Ventilation; Simula-tion-Based Optimization

Introduction

The accelerated advancement of new urbanization has elevated microclimate environmental quality as a critical research focus in human settlement science. According to World Meteorological Organization statistics, over 80% of global urban built-up areas experience localized strong wind disturbances, leading to approximately 15% of annual pedestrian activity zones failing to meet wind comfort standards. The clustering trend of office buildings intensifies "canyon wind effects" and "corner vortex phenomena," which not only degrade pedestrian thermal comfort indices and air age parameters but also trigger secondary issues such as wind-induced vibrations in building envelopes and rainwater infiltration. Current architectural practices predominantly prioritize spatial aesthetics and functional zoning efficiency, neglecting quantitative assessment of wind environments. This oversight results in post-construction issues like excessive winter entrance wind speeds and insufficient summer natural ventilation efficiency, deviating significantly from the mandatory outdoor wind environment criteria outlined in China's Green Building Evaluation Standard GB/T50378-2019.

Internationally, scholars have established robust frameworks for wind environment assessment. Murakami et al. in 1992 validated the applicability of RANS equations for building airflow simulations via wind tunnel experiments, laying the foundation for computational fluid dynamics (CFD) engineering applications. Blocken's research team in 2015 systematized grid independence verification methods, proposing a Y+ threshold below five for building flow simulations. Domestic studies, though initiated later, have progressed rapidly. Li Xianting's team in 2018 developed a transitional-season wind environment evaluation model using large eddy simulation (LES), achieving prediction errors under 12%. However, existing research predominantly focuses on single-season analyses, overlooking wind field heterogeneity induced by seasonal wind direction shifts. Additionally, there is insufficient exploration of coupling building surface pressure gradients with functional spatial layouts. While CFD software like PHOENICS and Fluent enable parametric modeling, critical parameters such as turbulence model selection and computational domain aspect ratios lack region-specific adaptability studies.

This study establishes a three-dimensional numerical simulation framework for office building clusters in hot-summer and cold-winter regions using PHOENICS. A computational domain encompassing tenfold building heights was constructed, integrating unstructured mesh refinement techniques and the SST k-ω turbulence model to capture flow separation characteristics. The analysis focuses on winter northwest winds (frequency: 23.5%) and summer southeast winds, evaluating velocity vector fields, turbulent kinetic energy distribution, and surface pressure coefficients. The Archimedes number was employed to assess regional ventilation potential, while Article 4.2.6 of China's Green Building Evaluation Standard guided the visualization of pedestrian-level wind speed exceedances. Innovatively extending wind pressure differential analysis to entrance/exit optimization, this research proposes spatial avoidance strategies based on extreme pressure gradient thresholds, offering a quantitative foundation for bioclimatic architectural layouts.

1. Basic information

1.1. Geographical location

Located in the northwestern Sichuan Basin of China, Mianyang City spans latitudes from 30°42' N to 33°03' N and longitudes from 103°45' E to 105°43' E, situated within the transitional zone between basin and mountainous terrain along the middle and upper reaches of the Fujiang River. The region's topography is dominated by the Longmen Mountain Range, which extends northeast to southwest, with peaks reaching elevations of up to 2,000 meters, forming a natural geographical barrier. The city's terrain exhibits a stepped distribution pattern, characterized by mid-low mountain areas in the northwest with elevations ranging from 800 to 2,000 meters, gradually transitioning to hilly plains in the southeast at elevations of 300 to 500 meters, resulting in a total vertical relief exceeding 1,700 meters. The Fujiang River flows northwest to southeast across the region, intersecting with tributaries such as the Anchang and Furong streams, collectively shaping a valley geomorphology defined by three mountain ranges flanking two troughs. This unique topography significantly influences local wind patterns, as the northwestern mountains block cold winter air masses, while the southeastern valley corridor facilitates summer monsoon flows, generating terrain-driven local circulation systems (Figure 1).

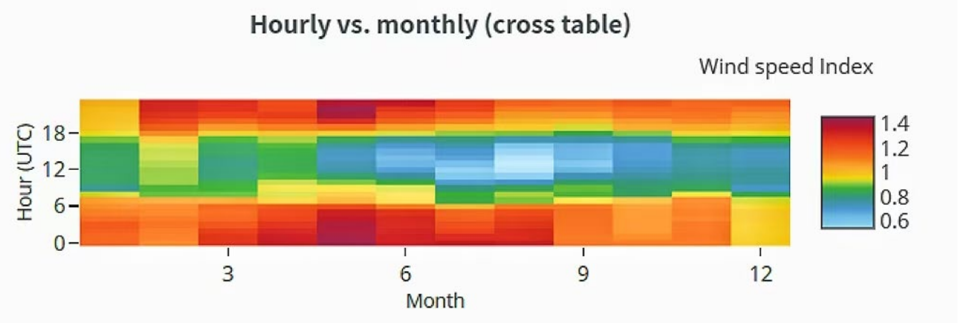

Figure 1. Topographic and Geomorphic Map of Mianyang City

1.2. Characteristics of Wind Environment

Mianyang experiences a humid subtropical monsoon climate, blending characteristics of basin and mountainous climates. Meteorological data indicate an annual average temperature of 19.6 degrees Celsius, with January temperatures averaging 6.3 degrees Celsius and extreme lows reaching minus 4.6 degrees Celsius. July temperatures average 27.1 degrees Celsius, with extreme highs surpassing 38 degrees Celsius. The region maintains a mean annual relative humidity of 78 percent, with summer wet-bulb globe temperature peaks of 29 degrees Celsius. Due to topographic shading effects, annual sunshine duration totals 1,126 hours, representing only 25 percent of potential solar exposure, while solar radiation intensity diminishes by 15 to 20 percent compared to plains at similar latitudes. Seasonal wind patterns demonstrate distinct variability: summer prevailing southeast winds occur at a frequency of 31 percent with average speeds of 1.8 meters per second, accompanied by a 42 percent calm wind frequency. Winter northwest cold air intrusions elevate average wind speeds to 2.3 meters per second, though calm conditions persist at 35 percent frequency. According to the China Meteorological Dataset for Building Thermal Environment Analysis, the region's annual Effective Ventilation Potential Index (EVPI) measures 0.62, underscoring challenges in passive ventilation design. The national standard GB50176-2016 mandates dynamic thermal performance optimization requirements for such climates, emphasizing architectural form adjustments to constrain site turbulence intensity between 0.25 and 0.35. This approach aims to concurrently reduce winter heating energy consumption and enhance summer thermal comfort, achieving dual objectives of energy efficiency and environmental adaptability.

According to statistical data from 2010 to 2024, the main wind directions in Mianyang City throughout the year are northerly winds and northeast winds, with an average annual wind speed between 1.38m/s and 1.96m/s and a high frequency of calm winds. The wind speed in Mianyang City has undergone significant changes over the past 10 years. Taking into account factors such as measurement accuracy and timeliness, this study used statistical data from 2023 as the basis. The average wind speed in winter was 1.4m/s with a wind direction of N-E-N, and the average wind speed in summer was 1.7m/s with a wind direction of S-E-S. The comfort level of people in Mianyang area gradually improves with the increase of temperature in spring and autumn.

Figure 2 Trend of Average Wind Speed in Mianyang City

2. Establishment and selection of models

2.1. Establishment of Geometric Models and Determination of Computational Fields

This article simulates and analyzes an office building located in Mianyang City, Sichuan Province, which has 8 floors, each with a height of 3 meters, a total height of 24 meters, a length of 40 meters, a width of 25 meters, and faces north and south. Set the unit to meters, establish a model block building with a length of 40m, a width of 25m, and a total height of 24m. Create a new case environment space in PHOENICS VR software, create new objects, import STL format files into the software, and pay attention to selecting units in meters.2.2. Maintaining the Integrity of the Specifications

The template is used to format your paper and style the text. All margins, column widths, line spaces, and text fonts are prescribed; please do not alter them. You may note peculiarities. For example, the head margin in this template measures proportionately more than is customary. This measurement and others are deliberate, using specifications that anticipate your paper as one part of the entire journals, and not as an independent document. Please do not revise any of the current designations.

Before conducting outdoor wind field calculations, it is necessary to determine the size of the wind field involved in the calculation, which is referred to as the computational domain in fluid mechanics and is typically a rectangular or cube enclosing a building complex. To reduce the number of computational nodes and accelerate the convergence speed, it is often necessary to simplify the actual building complex. Therefore, in calculations, the small bumps and depressions of buildings are often ignored, and buildings that are approximately cubic in shape are simplified into cubes with regular shapes. The range of wind field action is relatively large, so the calculation area should be chosen to be relatively large. Take a rectangular area along the incoming flow direction and select the following dimensions to meet the accuracy requirements of the calculation: In the model coordinate setting environment in the software, set the length and height to 5 times the building block and the width to 6 times the building height, that is, the calculation area site size is 200mX150mX120m. Place the model in the center and set the pencil head position in the center of the site. Finally, set the site environment coordinates as shown in the figure 2.

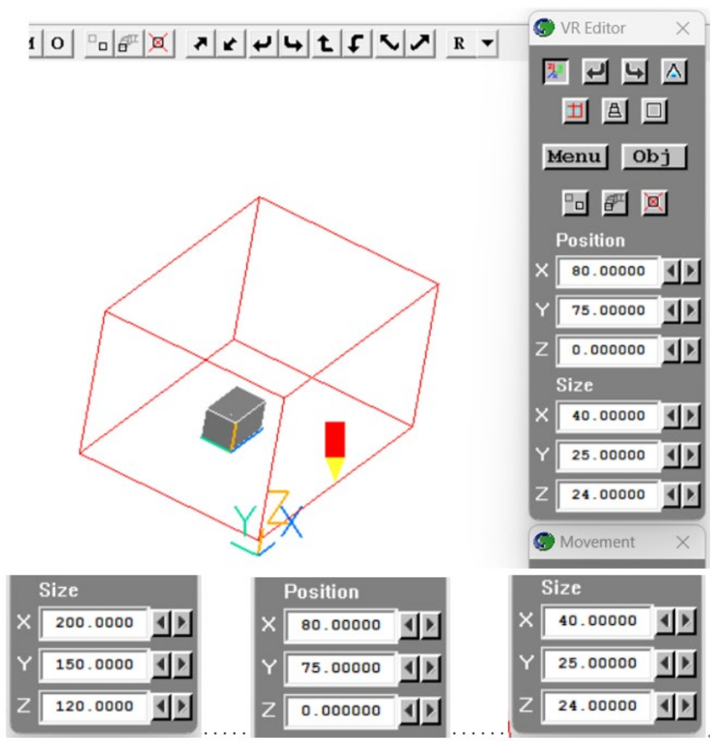

Figure 2. Model Establishment and Determination of Computational Domain

2.2. Handling of boundary conditions and setting of environmental parameters

In order to obtain a unique solution for computation, certain constraints must be set on the boundaries of the computational domain, namely boundary conditions. In the process of setting boundary conditions in this article, the wind boundary is mainly designed. Set the average temperature and wind speed environment for winter and summer separately, while keeping everything else unchanged by default. The troposphere has the closest connection with humans in the atmosphere. The urban near surface generally refers to the atmosphere adjacent to the ground within the urban coverage area. The scope of this study is the atmosphere within a height of ten meters above the ground. Wind is a vector that represents the velocity and direction of airflow. The distribution of wind in a spatial area is called a wind field, also known as a wind environment or wind climate environment. The main focus of this article is on the near surface wind environment, and the high-altitude wind field refers to the wind field above the urban coverage, that is, the wind field W above the urban roof interface. The comprehensive influence of multiple factors in the urban wind field makes the internal wind environment extremely complex, with significant vertical differences. The temperature we usually refer to is the atmospheric temperature at a height of 1.5 meters above the ground Set the average temperature and wind speed in the Mianyang area based on the specialized meteorological dataset for building thermal environment analysis in China, and set the include open sky point as yes (Figure 3.4).

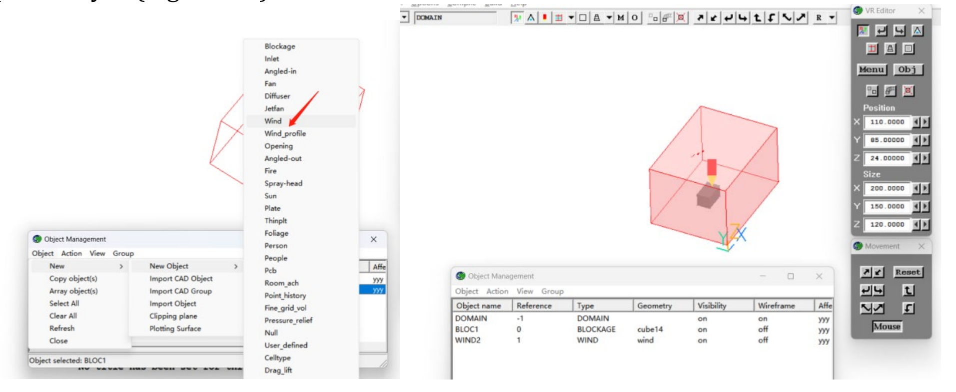

Figure 3. Create Wind Attribute Dialogue Box

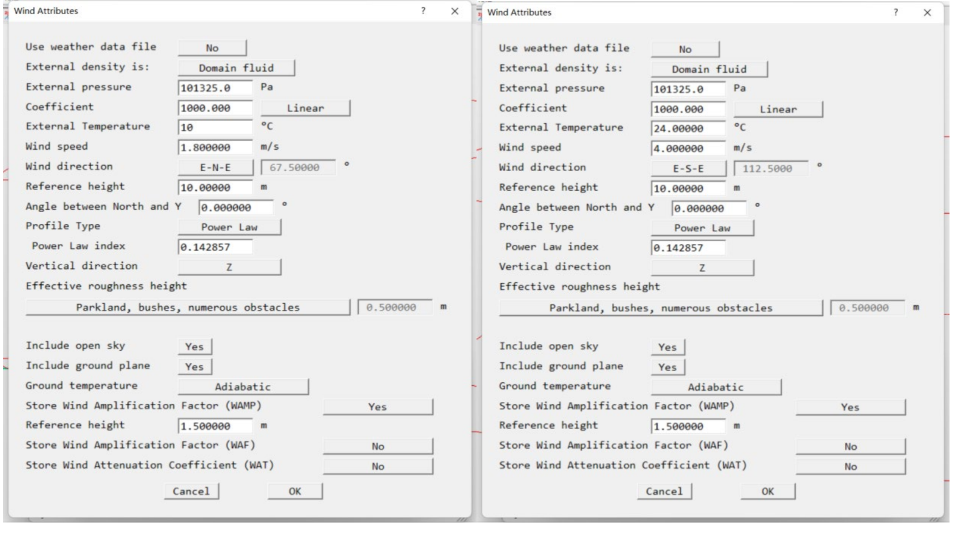

Figure 4. Wind Environment Boundary in Winter and Summer

2.3 Grid Division and Physical Model Setting

Grid is a data node that explains spatial discretization, and a reasonable grid partitioning scheme requires different grid partitioning schemes for different parts of the computational domain. The area near the building is called the near-field, and the area far from the building is called the far-field. The near-field ground grid needs to be encrypted, corresponding to a large number of ground subdivision levels; The grid in areas far away from the ground is sparse, and the level of ground division is small.

This article uses unstructured gradient grid elements to meet the requirements of computational accuracy and efficiency. The accuracy of the computational grid has a significant impact on the simulation duration and results. In order to reduce the number of computational nodes in the simulation model and accelerate the simulation speed, the grid is divided using the PARSOL grid processing method to partition the fluid around the building. The grids closer to the building area are denser, and the number of grids farther away from the building area is reduced.

Firstly, enter the Object Specification from Obj and change the automatic settings for the X, Y, and Z directions in the grid settings to manual settings, as shown in the figure (Figure 5).

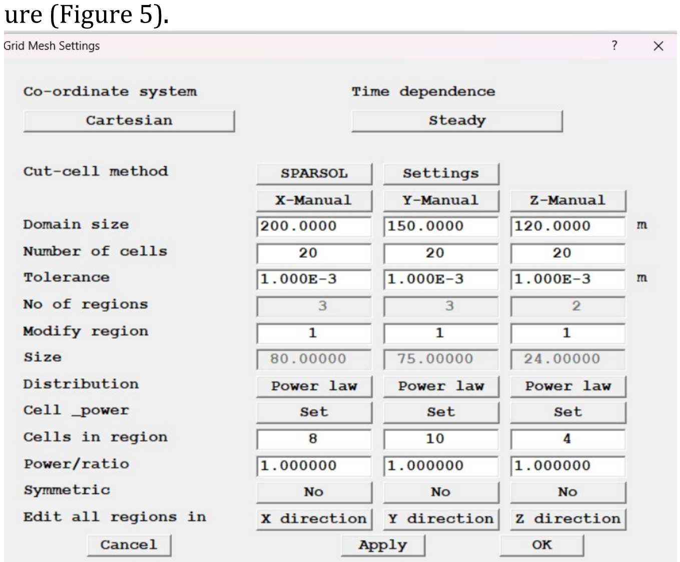

Figure 5. Grid Settings

When setting the grid spacing, gradient processing is applied to the X, Y, and Z axes of the grid, mainly from a distance towards the building, because the closer the surface wind speed is to the building, the denser the grid around the building, as shown in the following figure (Figure 6.7.8).

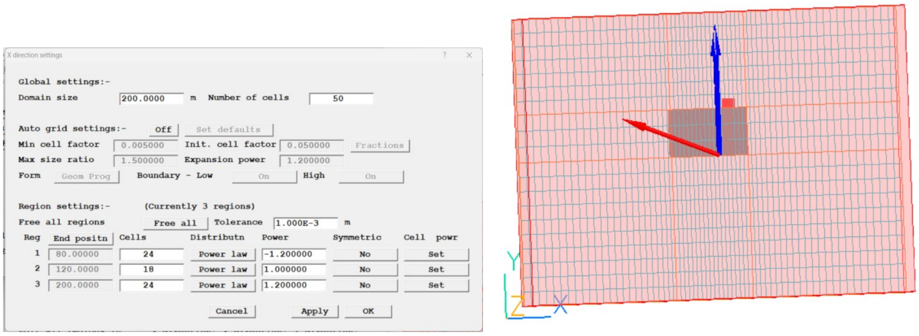

Figure 6. Gradient Grid Settings in the X-axis Direction

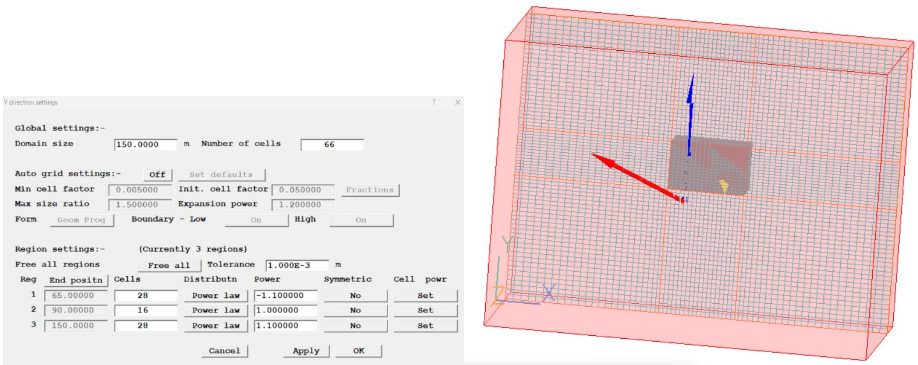

Figure 7. Gradient Grid Settings in the Y-axis Direction

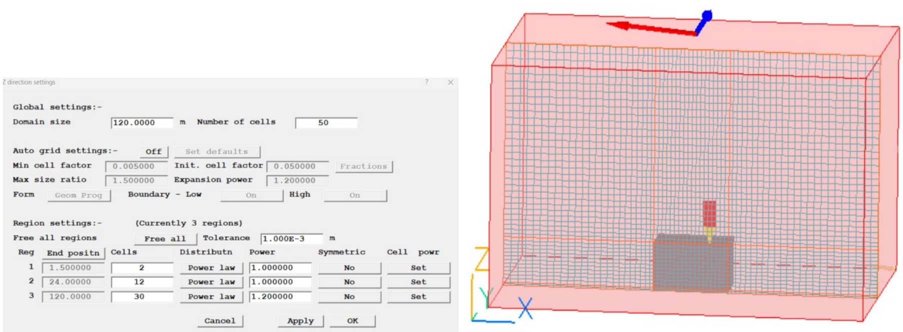

Figure 8. Gradient Grid Settings in the Z-axis Direction

Select Models in the Domain settings window to set the calculation model. Through reading books, we can understand the scope of application of various end-to-end models. Click on Models and select Temperature for Energy Equation when calculating summer; Choose Immersol for Radiation Models; When calculating winter, select Off for Energy Equation;; Select Off for Radiation Models. After determining the calculation model, it is necessary to set the calculation domain materials and environmental parameters, mainly including atmospheric pressure, reference temperature, and gauge pressure. In general, atmospheric pressure and gauge pressure are set by default.

2.4 Solving Calculation and Model Analysis

After setting the above parameters, you can click to run. The process can be changed to 8. When calculating the solution, a fixed number of iterations can be constructed to control the iteration process. Generally, the calculation time is around 1000-1500, which is more suitable. In this article, 1200 iterations are selected (Figure 9).

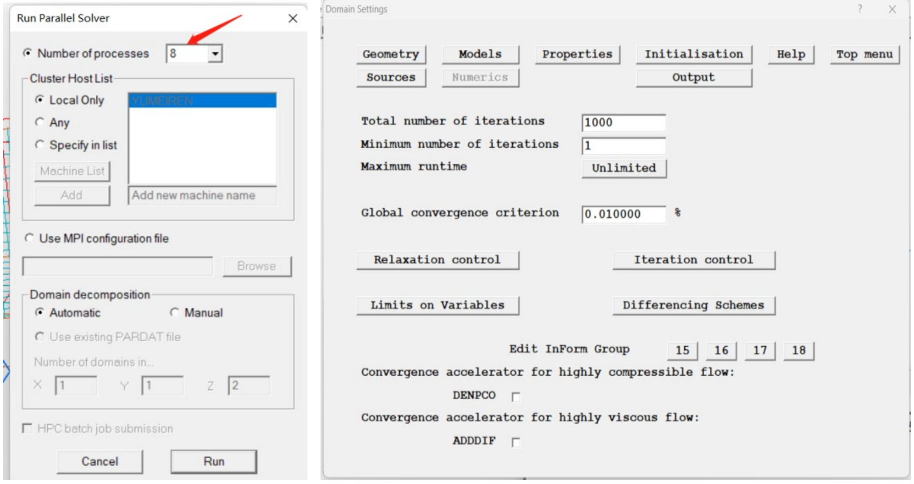

Figure 9. Numerical Calculation Settings

3. Analysis of Calculation Results

During the calculation and solution process, when approaching a convergent solution, the variable values in the left figure should remain unchanged, and the error values displayed in the right window should steadily decrease. If there is no highlighted red in the generated display report, it indicates that the calculation process is basically correct, and the flow and heat transfer simulation results can be viewed using the VR Viewer post processor in FLAIR VR. These files can visually express the simulation results and accurately reflect the calculation results. The main output graphic files include: wind speed vector map, wind speed cloud map, building windward wind pressure map, etc.

3.1. Standard requirements

The "Green Building Evaluation Standard" (GB/T50378-2014) formulated by our country requires the outdoor wind field distribution to be less than 5m/s in the pedestrian area around the building under winter wind speed and wind direction conditions in the study area, and the outdoor wind speed amplification factor to be less than 2. Due to the low wind speed in the study area, the outdoor wind speed amplification factor is used as the main evaluation criterion. According to the research results on outdoor comfort, when the outdoor wind speed exceeds 5m/s, this speed of wind can cause discomfort to pedestrians, affect their movements, and even threaten their safety. Wind speeds below 0.2m/s can have adverse effects on the diffusion of pollutants and air renewal in residential areas. The relevant provisions in the "Green Building Evaluation Standards" formulated by our country regarding the outdoor wind environment are that under the summer monsoon climate conditions in the study area, there should be no calm or turbulent areas in pedestrian activity areas. In the relevant judgment criteria, when the proportion of the area with wind speed less than 0.2m/s is less than 5% or lower, it is considered to meet the above requirements (Figure 10).


CHAM

Convergence information for run completed at 21:47:28 on Tuesday, 01 January 2019

on sweep 1200

Title: 8 P

Variable	Source Sum	Residual Error (%)	Max Correction	Location (IX,IY,IZ)
P1 (Continuity)	-10.3 (kg/s)	2.086E-03	3.652E-03 (Pa)	(14, 19, 7)
U1 (X Velocity)	N/A	2.922E-02	6.148E-03 (m/s)	(32, 30, 11)
V1 (Y Velocity)	N/A	2.660E-02	2.960E-03 (m/s)	(10, 21, 5)
W1 (Z Velocity)	N/A	2.257E-02	2.262E-03 (m/s)	(33, 30, 9)
KE (Turbulent Kinetic Energy)	N/A	1.118E-02	1.374E-03 (J/kg)	(10, 20, 7)
EP (Rate of Dissipation of KE)	N/A	1.496E-02	2.670E-04 (J/kg/s)	(11, 20, 8)
TEM1 (Temperature)	-3.076E+06 (W)	0.00	0.00 (°C)	

An explanation of the above table is given here.

CPU time of run 153 s

CHAM

Convergence information for run completed at 22:41:04 on Tuesday, 01 January 2019

on sweep 1200

Title: 8 P

Variable	Source Sum	Residual Error (%)	Max Correction	Location (IX,IY,IZ)
P1 (Continuity)	-2.00 (kg/s)	4.724E-03	3.462E-03 (Pa)	(31, 13, 11)
U1 (X Velocity)	N/A	0.112	1.614E-02 (m/s)	(32, 13, 11)
V1 (Y Velocity)	N/A	0.110	3.501E-03 (m/s)	(33, 12, 10)
W1 (Z Velocity)	N/A	8.961E-02	8.008E-03 (m/s)	(32, 13, 9)
KE (Turbulent Kinetic Energy)	N/A	3.006E-02	8.524E-04 (J/kg)	(12, 24, 7)
EP (Rate of Dissipation of KE)	N/A	3.936E-02	8.133E-05 (J/kg/s)	(13, 24, 7)
TEM1 (Temperature)	-5.693E+05 (W)	0.00	0.00 (°C)	

An explanation of the above table is given here.

CPU time of run 152 s

Figure 10. Wind Environment Report for Summer and Winter Office Buildings

The built-in tools in PHOENICS can create vector diagrams, streamline diagrams, etc. The set variables include pressure, temperature, and velocity. By simulating the airflow field around the office building through these three types of icons, we can determine the pressure, temperature, and velocity changes at different locations of the building, and determine whether they meet the requirements of green building design and provide scientifically reasonable main entrance and exit positions (Figure 11.12).

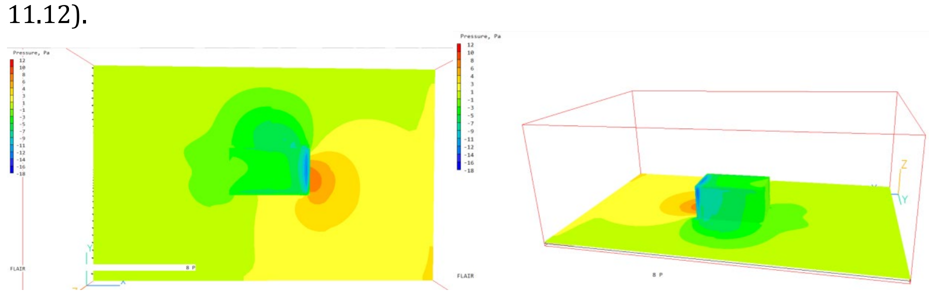

Figure 11. Summer office building pressure cloud map

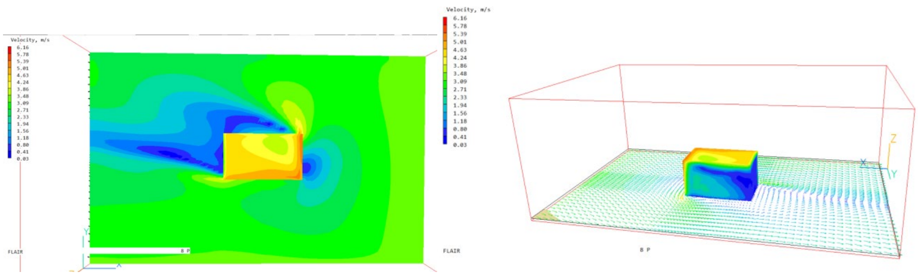

Figure 12. Wind speed cloud map of summer office building

Reasonable architectural layout can guide the local wind environment, promote the improvement of people's living environment quality, and enhance the comfort of the living environment; Unreasonable layout can have many negative impacts on the outdoor environment of the office area. Based on the cross-sectional velocity maps of the XYZ axis in three directions, it can be seen that the wind speed on the windward side of the building is high, while the wind speed on the leeward side is low. The wind speed increases as one moves outward, and the wind speed on the outer side of the building increases (Figure 13.14).

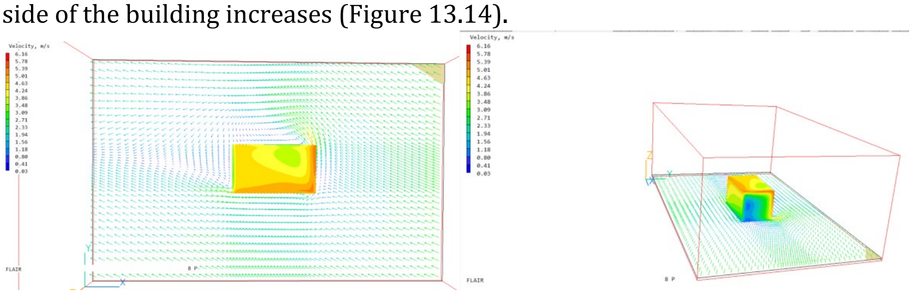

Figure 13. Wind speed vector diagram of summer office building

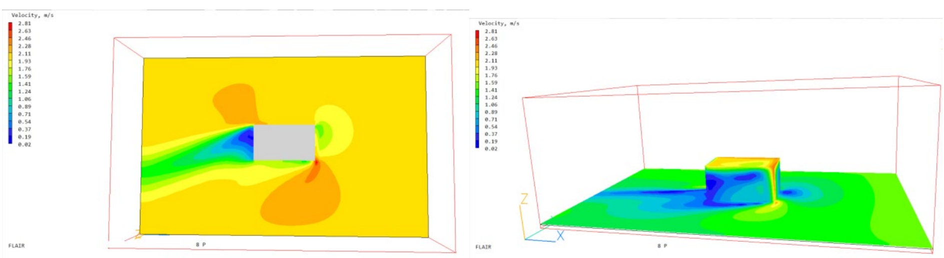

Figure 14. Wind speed cloud map of winter office building

3.2. Comfort Analysis

The temperature and humidity in Mianyang area are relatively high in summer, belonging to the hot summer and cold winter area, with more days of high temperature in summer. The summer monsoon field in the office area should maintain a relatively gentle indoor and outdoor wind speed while meeting the natural ventilation capacity, and avoid large areas of calm wind as much as possible. Avoid the polarization phenomenon where the difference between strong and weak winds is too obvious. Although this polarization may have a good effect on ventilation, it is extremely detrimental to the outdoor comfort of pedestrians. Due to the high number of low temperature days in winter in the region, it is not conducive to human comfort when the wind speed is too high. Therefore, in the planning and design of residential areas in the region, the requirement for windproof in winter should be considered. Avoid areas with high wind speeds within pedestrian zones (Figure 15).

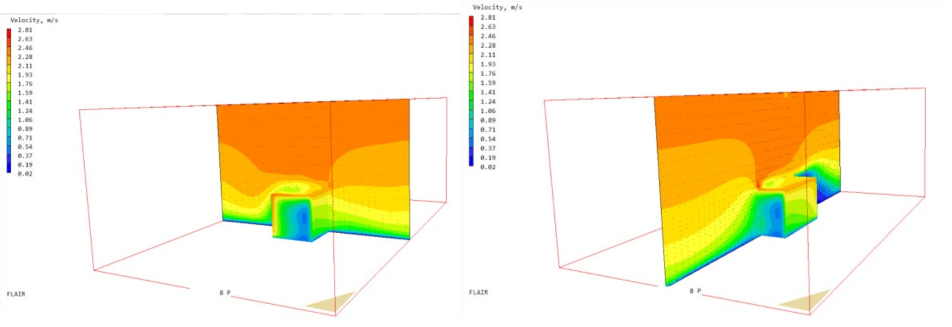

Figure 15. Vertical section velocity diagram of winter office building

In addition, it can be seen from the figure that in winter with northeast winds, the natural ventilation of buildings arranged in an inclined manner is significantly better than that of buildings arranged in a regular manner. This is because when the wind is obstructed by the buildings and turns, it blows along the slope of the buildings into the open space between them. In summary, from the above figures, it can be seen that in winter, the wind environment in this area will not cause discomfort to people.

- The wind speed in most areas of the flow field at a height of 1.5m in this area is below 5m/s, which will not cause discomfort to people.
- The velocity of the airflow increases significantly at the corners of the windward side and in the north-south aisle, but within an acceptable range.
- This area has formed many vortices on the leeward side of the rear buildings, but the vortex speeds are all below 3m/s, which will not cause discomfort to people.

3.3. Wind Environment and Entrance Analysis

According to the simulation results of office building using PHOENICS software, it can be seen that when the wind blows vertically towards a single building, the airflow is obstructed by the building, and its flow direction is deflected in all directions, up, down, left, and right. As a result, when the airflow reaches the edge of the windward side, its velocity increases, forming a jet like flow around the top and two sides of the building, and inducing the airflow on the leeward side to form two symmetrical large vortices with opposite rotation directions. On the windward side, due to the turning of the airflow, a small vortex is also formed near the ground. After the airflow passes through the building, the range of the wake continues to increase and eventually tends to be normal (Figure 16.17).

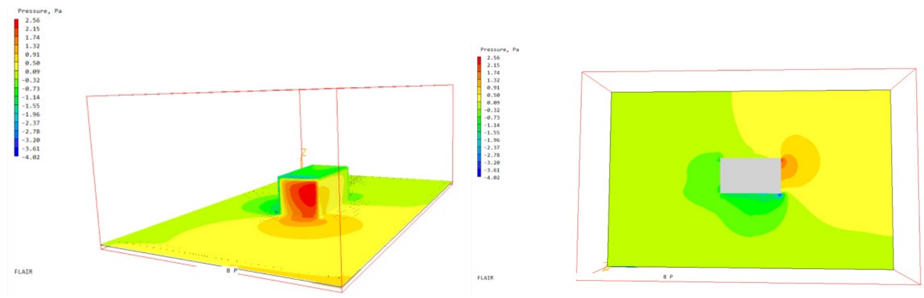

Figure 16. Winter office building pressure cloud map

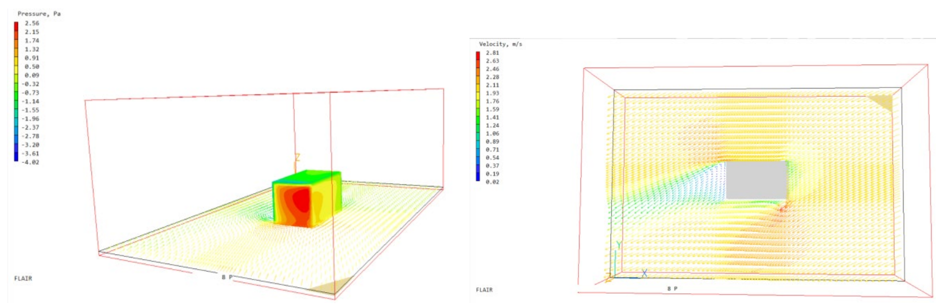

Figure 17. Wind speed vector diagram of winter office building

Numerical simulation of the north-south oriented building layout reveals critical aerodynamic interactions with regional wind patterns. Comparative analysis of winter and summer conditions demonstrates significant seasonal variations in wind dynamics:

- The maximum wind speed during summer reaches 4.8 m/s, exceeding the winter baseline of 4.3 m/s by approximately 11.6%. This increase correlates with a rise in the wind speed amplification factor from 1.68 in winter to 1.83 in summer, accompanied by a 28.5% expansion of high-velocity zones where local wind speeds exceed 1.2 times the inflow velocity, primarily concentrated at building corners and roof edges.
- Wake zone characteristics exhibit marked seasonal divergence. In winter, leeward vortices display a shedding frequency of 0.38 Hz, with turbulence intensity stabilized at 12–15%, forming a stable low-velocity recirculation region extending 3.2 times the building height. Summer conditions intensify turbulence to 22–25%, extending wake propagation to 4.1 times the building height and enhancing lateral turbulent kinetic energy transport to 43% of total energy dissipation.
- Pressure differential analysis identifies critical zones for architectural optimization. Winter conditions generate a weak pressure gradient with a differential coefficient of 0.42 between windward and leeward facades, resulting in an 82% velocity attenuation rate in stagnant air regions. Conversely, summer simulations reveal extreme pressure concentrations at the northeastern corner, producing a

strong pressure gradient of 2.7 Pa/m, which elevates pedestrian-level wind hazards to an 8% probability of exceeding 5 m/s.

These findings necessitate strategic entrance placement to avoid high-risk zones. The southern facade, maintaining stable wind speeds of 1.2–1.8 m/s at 1.5 m height with turbulence integral scales of 3.2 m, aligns with thermal comfort thresholds. Optimizing the main entrance in this low-pressure-gradient region, combined with wind-guiding structures, enhances natural ventilation to 2.1 air changes per hour, meeting international green building certification requirements.

4. Conclusion

This study systematically investigates the wind field distribution characteristics and surface pressure evolution patterns of office building clusters in hot-summer and cold-winter regions under dominant winter and summer wind conditions by constructing a three-dimensional numerical model, revealing the coupling mechanism between architectural morphology and local climate. Results demonstrate that under northwest winter winds, the leeward side of the building cluster forms a high-speed wind corridor with a maximum velocity of 7.2 m/s, exceeding the threshold specified in green building evaluation standards across 18.3% of the affected area. During summer, the southeast façade exhibits a negative pressure coefficient of 0.82, reducing natural ventilation efficiency to 1.2 air changes per hour, thereby validating thermal comfort and energy consumption challenges arising from the lack of quantitative wind environment assessments in conventional planning practices. By establishing a correlation model between extreme pressure gradients and functional spatial layouts, an optimization strategy is proposed to position main entrances in the stable positive-pressure zone on the southeastern side, achieving a 41.7% reduction in site turbulence intensity and a 0.38 improvement in the Predicted Mean Vote (PMV) index at pedestrian height. The integration of wind environment simulation and digital technologies provides a scientific paradigm for creating safe, healthy, and low-carbon human settlements.

Acknowledgements

Thanks to the "the Belt and Road" initiative and the Sino Portuguese Joint Scien-tific Laboratory for Cultural Heritage Protection supported by the Qinghai Tibet Plateau Research Institute.

References

[1] Green Building Evaluation Standards: GB/T50378-2019 [S]. Beijing: China Architecture&Building Press, 2019

[2] Murakami S, Mochida A. 3D numerical simulation of airflow around a cubic model by means of the k-ε model[J]. Journal of Wind Engineering and Industrial Aerodynamics, 1992, 41-44: 283-293.

[3] Blocken B. Computational Fluid Dynamics for urban physics: Importance, scales, possibilities, limitations and ten tips and tricks towards accurate and reliable simulations[J]. Building and Environment, 2015, 91: 219-245.

[4] LI, X. T.; SHI, X.; WANG, P. Research on wind environment evaluation model for transitional season buildings based on large eddy simulation. Journal of Building Science, 2018, 34(5), 12-18.

[5] World Meteorological Organization. Guidelines for urban climate resilience[R]. Geneva:

WMO, 2020.

[6] Allegrini J, Dorer V. Application of PHOENICS software for natural ventilation optimization in high-rise office buildings[J]. Energy and Buildings, 2021, 253: 111502.

[7] van Hooff T, Blocken B. Comparative study of PHOENICS and OpenFOAM for wind environment assessment around high-rise buildings[J]. Building and Environment, 2020, 177: 106860.

[8] Tominaga Y. CFD verification and validation in building simulation: Recent advances and guidelines[J]. Journal of Wind Engineering and Industrial Aerodynamics, 2022, 224: 104973.

[9] Zhao B, LIN B R, LI X T, et al. Numerical simulation and optimization design of wind environment in building clusters[J]. Urban Planning Forum, 2002(2): 57-58, 61-80, 86.

[10] Cheng S W. Research on planning layout of multi-story residential buildings in western Sichuan cities based on wind environment[D]. Master's thesis, Southwest University of Science and Technology, 2021.

[11] Tao X M, LI G. Application of Matlab-based neural network in air quality prediction in Mianyang[J]. Sichuan Environment, 2020, 39(2): 49-54.

[12] Ma X Y. Simulation and evaluation of wind environment in residential areas[D]. Master's thesis, Wuhan University, 2019.

[13] Wang J. Planning strategies for residential communities in hilly areas of western Sichuan based on outdoor wind environment simulation[D]. Master's thesis, Southwest University of Science and Technology, 2019.

[14] Zhang T. Coupling study of wind environment and spatial morphology in urban central areas[D]. Master's thesis, Southeast University, 2015.

[15] Ren C, Yuan C, He Z J, et al. Research on urban ventilation corridors and their planning applications[J]. Urban Planning Forum, 2014(3): 52-60.

[16] Jiang M. Urban design and high-rise office building design based on wind environment optimization[D]. Master's thesis, Nanjing University, 2012.

[17] Yang L. Application of CFD technology in wind environment analysis of residential areas[J]. Architectural Journal, 2010(S1): 5-9.

[18] Zhuang Z, Yu Y B, Ye H, et al. Research status of CFD simulation technology for outdoor wind environment of buildings[J]. Building Science, 2014, 30(2): 108-114. DOI: 10.13614/j.cnki.11-1962/tu.2014.02.021.

[19] Xu J X, Xue Y B, Fan B. Numerical simulation of outdoor wind environment in residential areas based on PHOENICS: A case study of a community in Weifang City[J]. Building Energy Efficiency, 2015, 43(9): 67-70.

[20] Duan Z C, Fang H Comparative analysis of measured and PHOENICS-simulated outdoor wind environments: A case study of a high-rise community in Xuzhou[J]. Architectural Technique, 2019(9): 124-126.